

## 2-D Columnar Assemblies of Diblock Rod-Coil Molecules Incorporating Cholesteryl Group

YANG LIU<sup>†</sup>, YIRONG PEI<sup>†</sup>, ZHUOSHI WANG, JUNJIE CUI, TIE CHEN<sup>\*</sup>, JINGZHE XU and LONG YI JIN<sup>\*</sup>

Key Laboratory for Organism Resources of the Changbai Mountain and Functional Molecules, Ministry of Education and Department of Chemistry, College of Science, Yanbian University, No. 977 Gongyuan Road, Yanji 133002, P.R. China

\*Corresponding authors: E-mail: tchen@ybu.edu.cn; lyjin@ybu.edu.cn

<sup>†</sup>These authors contributed equally to this work

Received: 9 July 2013;

Accepted: 10 September 2013;

Published online: 15 February 2014;

AJC-14714

Rod-coil molecules have a strong tendency to self-organize into supra-molecular nanostructures in the bulk state. In this article, we report synthesis and self-assembling behaviour of rod-coil molecules **1-3**, consisting of a biphenyl and cholesteryl group as a rod segment and poly(ethylene oxide) (PEO) with a degree of polymerization of 7, 12 and 17 coil segments. Self-organization behaviour of these molecules investigated by means of differential scanning calorimetry, thermal polarizing optical microscopy and small-angle X-ray scattering in the bulk state reveal that volume fraction of PEO coil segments containing alkyl chain of cholesteryl group dramatically influence the self assembling behaviour of rod building block in the liquid crystalline phase. Molecules **1-3** self-assemble into 1-D bilayered structures with different d-spacing according to the lengths of coil domains in the solid state. While, self-organized molecular structures transfer into oblique columnar structure for molecule **1** and **2** from the crystalline to the liquid crystalline phase, further increasing coil to rod volume fraction, molecule **3** self assemble into hexagonal columnar aggregate through  $\pi$ - $\pi$  stacking of rod building blocks.

**Keywords:** Self-assembly, Rod-coil, Small-angle X-ray scattering, Cholesteryl, 2-D Columnar.

### INTRODUCTION

A considerable amount of research has been done to control the supramolecular structures with well-defined shapes and sizes which have potential for fundamental and practical implications in areas such as materials science, molecular electronics and biomimetic chemistry<sup>1-6</sup>. Recently, functionalized rod-coil molecules have been studied by researchers for construction of nano-scale materials with potential electro-photo properties<sup>7-13</sup>. Self-assembly of rod-coil block molecules provide various supramolecular nanostructures from 1-D lamellar, 2-D columnar, 3-D bundles in the bulk state, through non-covalent forces including hydrophobic and hydrophilic effects, electrostatic interaction, hydrogen bonding and micro-phase segregation<sup>14-23</sup>. It has been reported that molecular parameters such as volume fraction of rod to coil segment, the cross-sectional area of coil segment, the shape of rigid rod segment dramatically influence driving force of molecules to form various nanostructure<sup>24-27</sup>. Cholesterol-substituted molecules have strong tendency to self-assemble into twisted helical aggregations with distinct optical, chiroptical properties<sup>28-33</sup>. Hence, it is growing interest in the design of synthetic rod-coil molecules incorporating cholesteryl block that are able to self-assemble into diverse supramolecular nanostructures for application in nano-wire and materials science.

With this in mind, we synthesized rod-coil molecules containing cholesteryl group as a part of rod segment and poly(ethylene oxide) with a degree of polymerization of 7, 12 and 17 linked together with biphenyl group as coil segments (**Scheme-I**). The self-assembling behaviours of these molecules investigated by using differential scanning calorimetry (DSC), thermal polarizing optical microscopy (POM) and small-angle X-ray scatterings (SAXS) in the bulk state.

### EXPERIMENTAL

4,4'-Biphenol, poly(ethylene glycol) methyl ether ( $M_w = 350, 550, 750$ ), toluene-*p*-sulfonyl chloride (TsCl, 99 %), cholesteryl chloroformate, pyridine, potassium carbonate, triethylamine (99.5 %) and conventional reagents were used as received. Compounds **4-6** and **7-9** were prepared according to the similar procedures described elsewhere<sup>12,13</sup>.

**Techniques:** <sup>1</sup>H NMR spectra was recorded from CDCl<sub>3</sub> solution on a Bruker AM 300 spectrometer. A Perkin Elmer Pyris Diamond differential scanning calorimeter was used to determine the thermal transitions with the maxima and minima of their endothermic or exothermic peaks, controlling the heating and cooling rates to 10 °C min<sup>-1</sup>. X-Ray scattering measurements were performed in transmission mode with synchrotron radiation at the 1W2A X-ray beam line at Beijing Accelerator Laboratory, China and at the 3C2 X-ray beam line at Pohang

Accelerator Laboratory, Korea. MALDI TOF-MS was performed on a Perceptive Biosystems Voyager-DE STR using a 2-cyano-3-(4-hydroxyphenyl) acrylic acid (CHCA) as matrix. A Olympus optical polarized microscope equipped with a Mettler FP 82 hot-stage and a Mettler FP 90 central processor was used to observe the thermal transitions and to analyze the anisotropic texture.

**Synthesis of molecules 1-3:** Molecules **1-3** were synthesized using the similar procedures. A representative example is described for **1**. A mixture of compound **7** (0.83 g, 1.55 mmol) and cholesteryl chloroformate (2.0 g, 7.7 mmol) were dissolved in absolute toluene (40 mL) in a 100 mL two-neck flask adding triethylamine (3 mL) as catalyst, then refluxed for 24 h. The solvent was removed in a rotary evaporator and the crude product was purified by column chromatography on silica gel using  $\text{CH}_2\text{Cl}_2$ , ethyl acetate and ethyl acetate: MeOH (20:1) as eluent to yield 0.9 g of yellow wax-like solid (70 %).  $^1\text{H NMR}$  (300 MHz,  $\text{CDCl}_3$ ,  $\delta$ , ppm) 7.46-7.55 (m, 4Ar-H, m to phenyl-OCO, m to  $\text{CH}_2\text{O}$  phenyl), 7.22 (d, 2Ar-H, o to phenyl-OCO,  $J = 9.0\text{ Hz}$ ), 6.97 (d, 2Ar-H, O to  $\text{CH}_2\text{O}$  phenyl,  $J = 9.0\text{ Hz}$ ), 5.42 (t, 1H, C=CH,  $J = 5.1\text{ Hz}$ ), 4.54-4.67 (m, 1H, OCH), 4.17 (t, 2H, phenyl  $\text{OCH}_2\text{CH}_2\text{O}$ ,  $J = 4.8\text{ Hz}$ ), 3.88 (t, 2H, phenyl  $\text{OCH}_2\text{CH}_2\text{O}$ ,  $J = 4.8\text{ Hz}$ ), 3.54-3.74 (m, 24 H,  $-\text{OCH}_2\text{CH}_2\text{O}$ ), 3.38 (s, 3H,  $\text{OCH}_3$ ), 0.68-2.51 (m, 46H, cholesteryl part); MALDI-TOF-MS  $m/z$  [ $\text{M}$ ] $^+$  995.

**Molecule 2:** Yield 73 %.  $^1\text{H NMR}$  (300 MHz,  $\text{CDCl}_3$ ,  $\delta$ , ppm) 7.46-7.55 (m, 4Ar-H, m to phenyl-OCO, m to  $\text{CH}_2\text{O}$  phenyl), 7.22 (d, 2Ar-H, o to phenyl-OCO,  $J = 9.0\text{ Hz}$ ), 6.98 (d, 2Ar-H, o to  $\text{CH}_2\text{O}$  phenyl,  $J = 9.0\text{ Hz}$ ), 5.42 (t, 1H, C=CH,  $J = 4.8\text{ Hz}$ ), 4.54-4.65 (m, 1H, OCH), 4.17 (t, 2H, phenyl  $\text{OCH}_2\text{CH}_2\text{O}$ ,  $J = 4.8\text{ Hz}$ ), 3.88 (t, 2H, phenyl  $\text{OCH}_2\text{CH}_2\text{O}$ ,  $J = 4.8\text{ Hz}$ ), 3.64-3.73 (m, 46H,  $-\text{OCH}_2\text{CH}_2\text{O}$ ), 3.38 (s, 3H,  $\text{OCH}_3$ ), 0.69-2.51 (m, 46H, cholesteryl part); MALDI-TOF-MS  $m/z$  [ $\text{M}$ ] $^+$  1127.

**Molecule 3:** Yield 71 %.  $^1\text{H NMR}$  (300 MHz,  $\text{CDCl}_3$ ,  $\delta$ , ppm) 7.46-7.55 (m, 4Ar-H, m to phenyl-OCO, m to  $\text{CH}_2\text{O}$  phenyl), 7.22 (d, 2Ar-H, O to phenyl-OCO,  $J = 9.0\text{ Hz}$ ), 6.98 (d, 2Ar-H, O to  $\text{CH}_2\text{O}$  phenyl,  $J = 9.0\text{ Hz}$ ), 5.42 (t, 1H, C=CH,

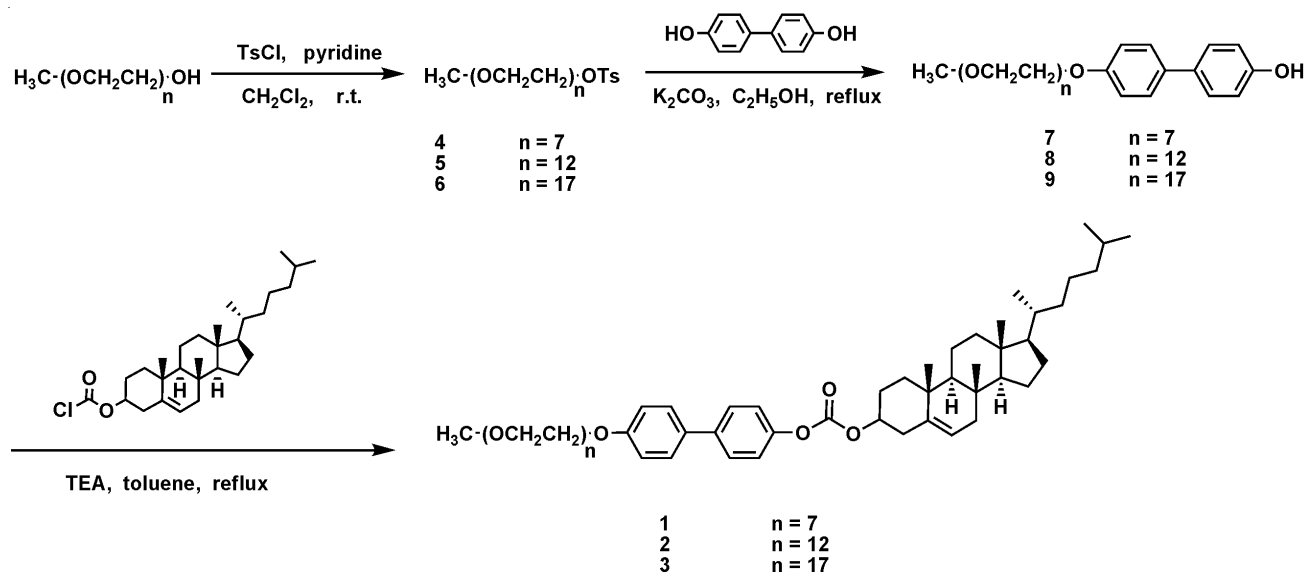
$J = 4.8\text{ Hz}$ ), 4.54-4.65 (m, 1H, OCH), 4.17 (t, 2H, phenyl  $\text{OCH}_2\text{CH}_2\text{O}$ ,  $J = 4.8\text{ Hz}$ ), 3.88 (t, 2H, phenyl  $\text{OCH}_2\text{CH}_2\text{O}$ ,  $J = 4.8\text{ Hz}$ ), 3.53-3.74 (m, 70H,  $-\text{OCH}_2\text{CH}_2\text{O}$ ), 3.38 (s, 3H,  $\text{OCH}_3$ ), 0.69-2.51 (cholesteryl part); MALDI-TOF-MS  $m/z$  [ $\text{M}$ ] $^+$  1347.

## RESULTS AND DISCUSSION

**Synthesis of molecules 1-3:** Rod-coil molecules containing cholesteryl group as a part of rod segment and poly(ethylene oxide) with a degree of polymerization of 7, 12 and 17 linked together with biphenyl group as coil segments were synthesized using 4,4'-biphenol and poly(ethylene glycol) methyl ethers as starting materials. Molecules **1-3** were obtained by nucleophilic substitution reaction of cholesteryl chloroformate and compound **7-9** in the presence of triethylamine as catalyst (**Scheme-I**). The structures of these molecules were characterized by  $^1\text{H NMR}$  spectroscopy (Fig. 1) and matrix-assisted laser desorption ionization time-of-flight (MALDI-TOF) mass spectroscopy (Fig. 2) were shown to be in full agreement with the structures presented in **Scheme-I**.

**Structure analysis in the bulk state:** The self-assembling behaviour of **1-3** was investigated by means of differential scanning calorimetry (DSC), thermal polarizing optical microscopy (POM) and X-ray diffraction (XRD) in the bulk state. Fig. 3 shows the DSC heating and cooling traces of molecules **1-3** and exhibited their thermotropic liquid crystalline phase at 64, 58 and 47 °C. On further increasing temperature, the isotropic liquid phase was observed at 130, 113 and 76 °C, respectively. Similar to conventional linear rod-coil molecules, the melting transition temperatures of the rod-coil diblock oligomers **1-3** increase as the poly(ethylene oxide) coil length decrease<sup>3,5,12</sup>.

On slow cooling of **1-3** from isotropic liquid to liquid-crystalline mesophase, focal conic textures were observed on optical polarize microscope, indicating the presence of the 2-D columnar liquid-crystalline mesophases (Fig. 4). Especially, molecule **3** exhibited the pseudo focal conic texture in the POM experiment which is indicative of existence of hexagonal columnar structure (Fig. 4c).



**Scheme-I:** Synthetic route of molecules **1**, **2** and **3**

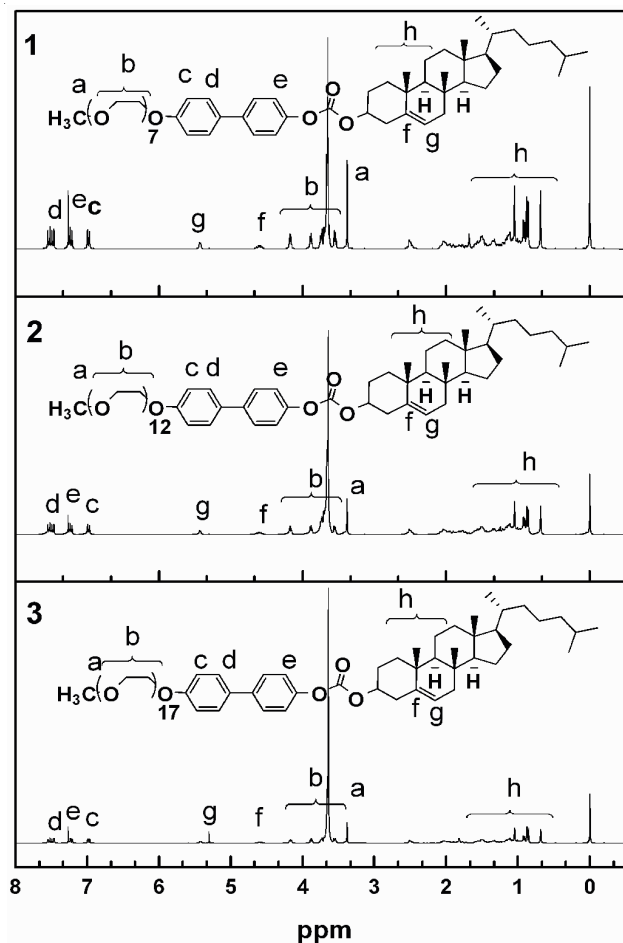


Fig. 1.  $^1\text{H}$  NMR spectra of molecules **1**, **2** and **3** (solvent:  $\text{CDCl}_3$ )

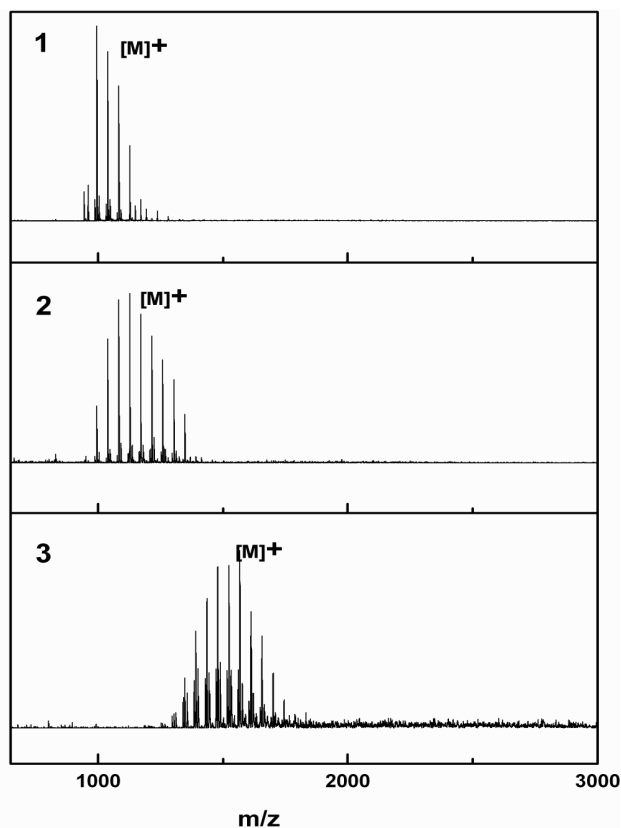


Fig. 2. MALDI-TOF-MS spectra of molecules **1**, **2** and **3** (matrix: CHCA).

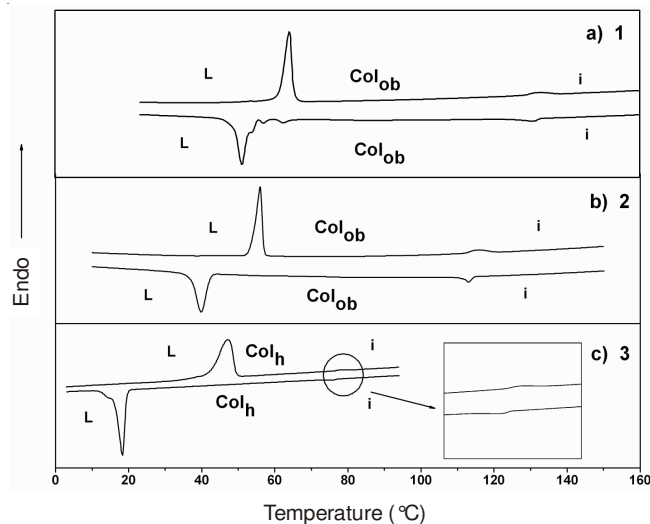


Fig. 3. DSC traces ( $10\text{ }^\circ\text{C min}^{-1}$ ) recorded for heating and the cooling scans of **1**, **2** and **3**

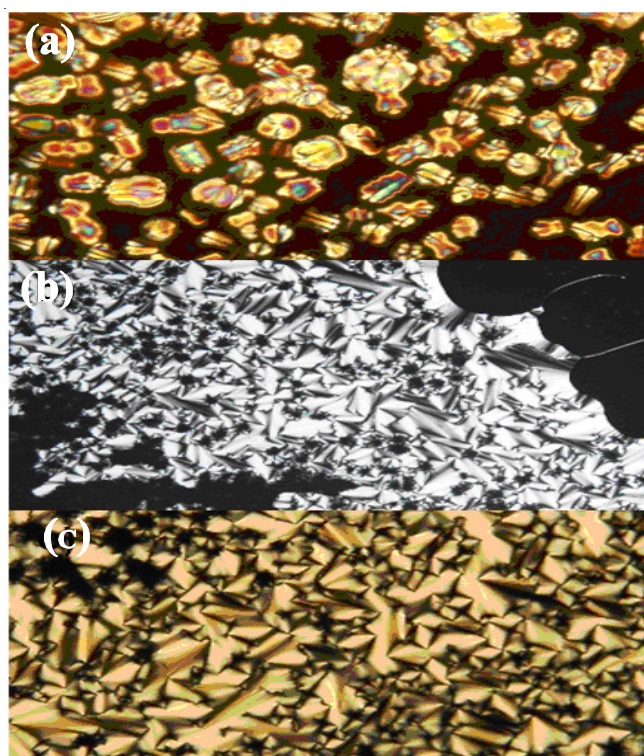


Fig. 4. Representative POM micrograph ( $\times 40$ ) of the textures exhibited by (a) an oblique columnar structure of **1**; (b) an oblique columnar structure of **2** and (c) a hexagonal columnar structure of **3** at the transition from the isotropic liquid

To identify the detailed self-organizing structures in the bulk state, X-ray scattering experiments of molecules **1-3** were performed at various temperatures. Figs. 5a and 6a show X-ray diffraction patterns for compound **1** recorded at 35 and  $110\text{ }^\circ\text{C}$  on cooling from the isotropic phase to the liquid-crystalline phase. In the solid state, several peaks corresponding to equidistant  $q$ -spacings in the small-angle region can be indexed as the (001), (002) and (003) reflections for a 1-D lamellar phase. A layer spacing ( $d$ -spacing) of 7.62 nm is calculated from the (001) plane, which is larger than the corresponding estimated molecular length 5.75 nm (by Corey-Pauling-Koltun

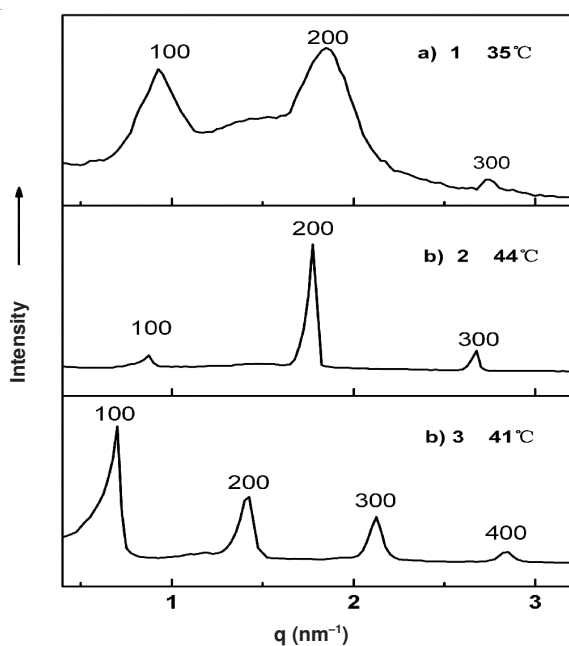


Fig. 5. X-Ray diffraction patterns of lamellar structure for molecules **1**, **2** and **3** measured at solid state

(CPK) molecular modeling). It can be explained that molecule **1** formed a bilayered lamellar structure in the solid state, in which the hydrophobic and PEO segments are fully overlapped. In the liquid-crystalline phase, the small-angle X-ray diffraction pattern of **1** measured at 110 °C shows four reflections. These reflections can be indexed as the (100), (110), (010) and (200) planes (Fig. 6a) for a two-dimensional oblique columnar structure with a characteristic angle  $\gamma = 60^\circ$  and lattice parameters  $a = 6.38$  nm,  $b = 4.17$  nm (Table-1). To further investigate inner packing arrangement of molecule **1**, we performed wide-angle X-ray scattering experiment. A broad single peak centered at approximately 0.514 nm in the wide-angle region indicative of liquid-crystalline ordering of the aromatic segments within the rod domains. Based on the experimental values of the unit cell parameters ( $a = 6.38$  nm,  $b = 4.17$  nm,  $c = 0.514$  nm and  $\gamma = 60^\circ$ ) and the density of **1** ( $\rho = 1.04$ ), the number of molecules in a single slice of the column is calculated about 8, according to the following equation, where  $M$  is the molecular weight and  $N_A$  is Avogadro's number.

$$n = (\text{abcsin}\gamma)\rho N_A/M \quad (1)$$

Similar to molecule **1**, in the solid state, XRD experiments of molecule **2** and **3** display several peaks corresponding to equidistant  $q$ -spacings in the small-angle region, that also can be indexed as the (001), (002) and (003) or (004) reflections for the 1-D lamellar phases. The layers spacing are about 8.05 nm and 10.07 nm calculated from the (001) plane, which are also larger than the corresponding estimated molecular length 7.65 nm and 9.45 nm respectively, indicative of self-organizing into bilayered lamellar structure in the solid state (Figs. 5b, 5c).

Compared with molecule **1**, molecule **2** with a longer coil segments give rise to slight change to the structure of liquid-crystalline phase. Fig. 6b shows X-ray diffraction patterns for molecule **2** recorded at 95 °C, several diffraction patterns corresponding in the small-angle region also can be indexed as the (100), (110), (010) and (200) planes for a two-dimen-

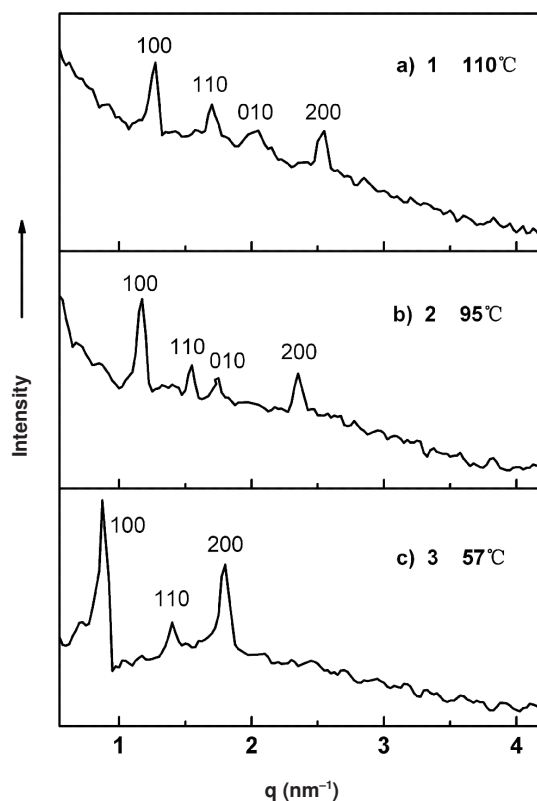


Fig. 6. SAXS patterns of **1**, **2** and **3** measured in the liquid-crystalline state, plotted against  $q (= 4\pi \sin \theta/\lambda)$ : (a) oblique columnar for **1** at 110 °C; (b) oblique columnar phase for **2** at 95 °C; (c) hexagonal columnar for **3** at 57 °C.

TABLE-1  
SAXS DATA FOR AN OBLIQUE COLUMNAR STRUCTURE OF **1**, IN THE LIQUID CRYSTALLINE PHASE

h	k	l	$q_{\text{obsd}} (\text{nm}^{-1})$	$q_{\text{calcd}} (\text{nm}^{-1})$
1	0	0	1.1323	1.1323
1	1	0	1.538	1.5334
0	1	0	1.7386	1.7386
2	0	0	2.2733	2.2733

$q_{\text{obs}}$  and  $q_{\text{calc}}$  are the scattering vectors of the observed and calculated reflections for the oblique columnar structure with lattice parameters  $a = 6.38$  nm,  $b = 4.173$  nm and  $\gamma = 60^\circ$ .

sional oblique columnar structure with a characteristic angle  $\gamma = 61^\circ$  and lattice parameters  $a = 6.86$  nm,  $b = 4.59$  nm. With regard to molecule **2**, the elongated chain magnifies the space crowding thus leading to increasing the lattice parameters of oblique columnar structure (Table-2). The number of molecules of **2** in a single slice of the column is about 8 calculated according the equation 1.

TABLE-2  
SAXS DATA FOR AN OBLIQUE COLUMNAR STRUCTURE OF **2**, IN THE LIQUID CRYSTALLINE PHASE

h	k	l	$q_{\text{obsd}} (\text{nm}^{-1})$	$q_{\text{calcd}} (\text{nm}^{-1})$
1	0	0	1.0431	1.0431
1	1	0	1.3819	1.3819
0	1	0	1.5343	1.5334
2	0	0	2.0950	2.0950

$q_{\text{obs}}$  and  $q_{\text{calc}}$  are the scattering vectors of the observed and calculated reflections for the oblique columnar structure with lattice parameters  $a = 6.86$  nm,  $b = 4.585$  nm and  $\gamma = 61^\circ$ .

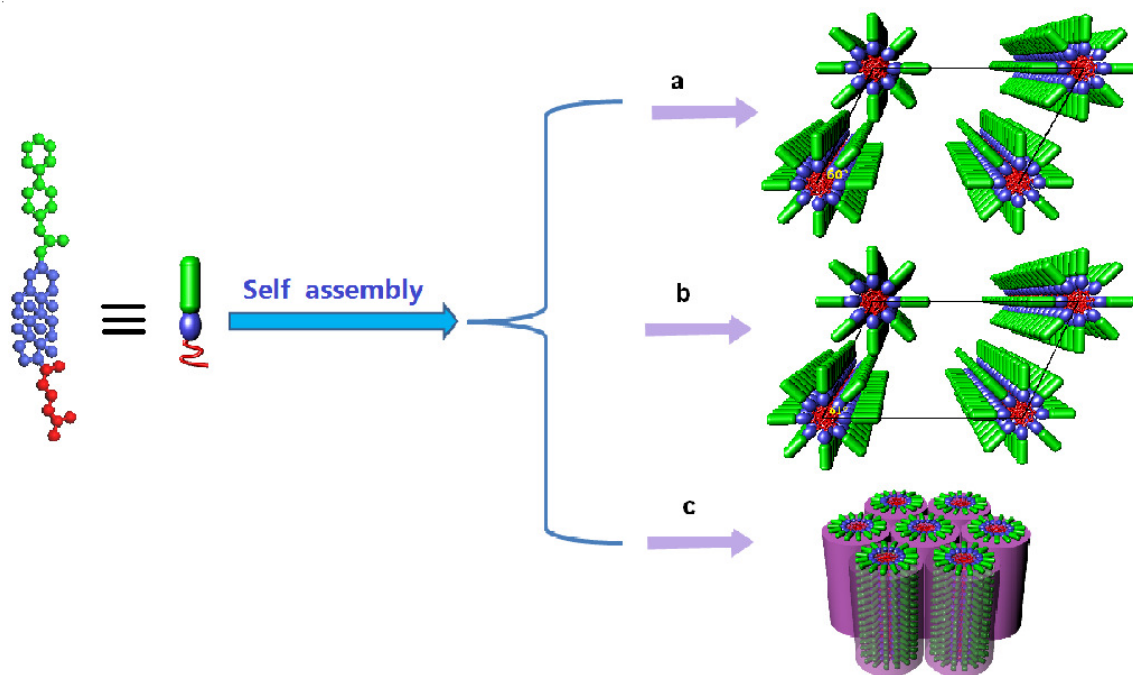


Fig. 7. Schematic representation of self-assembly of (a) an oblique columnar structure for **1**, (b) an oblique columnar structure for **2**, (c) hexagonal columnar for **3**

For molecule **3** with the longer poly(ethylene oxide) coil segment, the SAXS patterns in the melt state measured at 57 °C displays three peaks with the d-spacing ratio of 1:  $3^{1/2}$ : 2, which can be interpreted as a hexagonal columnar structure with a lattice constant  $a = 9.04$  nm. From characteristic of pseudo-focal conic domains shown by the POM, together with SAXS data of **3**, we confirmed that molecule **3** self-assemble into hexagonal columnar nanostructure in the liquid crystalline mesophase. These results indicate that parameters of the coil segments with different lengths of coil chains dramatically influence the self-assembly of block molecules as well as the cholesteryl alky unit, forming various supramolecular structure, from the lamellar structure to diverse columnar liquid-crystalline mesophases for molecules **1-3** (Table-3). Based upon the data presented so far, a schematic representation of the self-assembled structures of **1-3** is illustrated in Fig. 7.

TABLE-3  
CHARACTERIZATION OF THE THERMOTROPIC  
LIQUID-CRYSTALLINE BEHAVIOR OF  
MOLECULES IN THE BULK STATE

Molecule	Crystalline phase (lamellar)			Liquid-crystalline phase (columnar)			
	$f_{\text{coil}}$	$l$ (nm)	$d$ (nm)	$a$ (nm)	$b$ (nm)	$\gamma$ (°)	$n$
1	0.37	5.75	7.62	6.38	4.17	60	8
2	0.49	7.65	8.05	6.86	4.58	61	8
3	0.57	9.45	10.07	9.04	9.04	120	15

$a, b$ , lattice constants;  $\gamma$ , characteristic angle;  $n$ , number of molecules in a unit cell;  $d$ , layer spacing;

$f_{\text{coil}}$ , coil volume fraction;  $l$ , stretched molecular length

## Conclusion

Rod-coil molecules **1-3** consisting of a biphenyl as a rod segment and poly(ethylene oxide) with a degree of polymerization of 7, 12 and 17 coil segments connected to one side of

biphenyl and the other side with cholesteryl group were successfully synthesized. XRD studies in the crystalline phase reveal that these molecules self-organized into 1-D bilayered structures with different d-spacings according to the lengths of molecules. However, self-organized molecular structures transfer to various columnar structures in the liquid-crystalline phase. XRD experiments together with POM textures demonstrate that molecule **1** and **2** convert into oblique columnar structure. While, further increasing coil volume fraction, molecule **3** self assemble into hexagonal columnar aggregate, which have potentially application in materials science, molecular electronics and biomimetic chemistry.

## ACKNOWLEDGEMENTS

This work was supported by the National Natural Science Foundation of China (grant number: 21164013) and the Jilin Provincial Science and Technology Department (Grant number: 201115225). The authors are grateful to Institute of High Energy Physics, Chinese Academy of Sciences and Pohang Accelerator Laboratory, Korea for using Synchrotron Radiation Source.

## REFERENCES

1. A. Ajayaghosh, R. Varghese, S.J. George and C. Vijayakumar, *Angew. Chem. Int. Ed.*, **45**, 1141 (2006).
2. W. Jin, T. Fukushima, A. Kosaka, M. Niki, N. Ishii and T. Aida, *J. Am. Chem. Soc.*, **127**, 8284 (2005).
3. H.S. Jeong, Y.H. Kim, J.S. Lee, J.H. Kim, M. Srinivasarao and H.-T. Jung, *Adv. Mater.*, **24**, 381 (2012).
4. V. Percec, J.G. Rudick, M. Peterca and P.A. Heiney, *J. Am. Chem. Soc.*, **130**, 7503 (2008).
5. J. Lee, J. Kim, M. Yun, C. Park, J. Park, K.-H. Lee and C. Kim, *Soft Matter*, **7**, 7503 (2011).
6. H.-J. Kim, T. Kim and M. Lee, *Acc. Chem. Res.*, **44**, 72 (2011).
7. L. Liu, D.-J. Hong and M. Lee, *Langmuir*, **25**, 5061 (2009).
8. D.G.D. Patel, F. Feng, Y.-Ohnishi, K.A. Abboud, S. Hirata, K.S. Schanze and J.R. Reynolds, *J. Am. Chem. Soc.*, **134**, 2599 (2012).

9. T.L.D. Tam, W. Ye, H.H.R. Tan, F. Zhou, H. Su, S.G. Mhaisalkar and A.C. Grimsdale, *J. Org. Chem.*, **77**, 10035 (2012).
10. F.J.M. Hoeben, P. Jonkheijm, E.W. Meijer and A.P.H.J. Schenning, *Chem. Rev.*, **105**, 1491 (2005).
11. L.Y. Jin, J. Bae, J.H. Ryu and M. Lee, *Angew. Chem. Int. Ed.*, **45**, 650 (2006).
12. K.L. Zhong, Z. Huang, Z. Man, L.Y. Jin, B. Yin and M. Lee, *J. Polym. Sci. A, Polym. Chem.*, **48**, 1415 (2010).
13. L. Yi Jin, J. Bae, J.-H. Ahn and M. Lee, *Chem. Commun.*, 1197 (2005).
14. B.K. Cho, M. Lee, N.K. Oh and W.C. Zin, *J. Am. Chem. Soc.*, **123**, 9677 (2001).
15. H.A. Klok, J.F. Langenwalter and S. Lecommandoux, *Macromol.*, **33**, 7819 (2000).
16. E. Lee, Z. Huang, J. Ryu and M. Lee, *Chem. Eur. J.*, **14**, 6957 (2008).
17. K.L. Zhong, C.C. Yang, T. Chen, B.Z. Yin, L.Y. Jin, Z. Huang and E. Lee, *Macromol. Res.*, **18**, 289 (2010).
18. C.-H. Choi, J.-H. Lee, T.-S. Hwang, C.-S. Lee, Y.-G. Kim, Y.-H. Yang and K.M. Huh, *Macromol. Res.*, **18**, 254 (2010).
19. A. Ghosh and W.B. Lee, *Macromol. Res.*, **19**, 483 (2011).
20. L.Y. Jin, R. Hou, T. Chen, M. Fang, S. Mah and B. Yin, *Fibers Polymers*, **8**, 143 (2007).
21. K.L. Zhong, T. Chen, B.Z. Yin and L.Y. Jin, *Macromol. Res.*, **17**, 280 (2009).
22. L. Chen, K.L. Zhong, L.Y. Jin, Z.G. Huang, L. Liu and L.S. Hirst, *Macromol. Res.*, **18**, 800 (2010).
23. C.C. Yang, K.L. Zhong, Q. Wang, T. Chen and L.Y. Jin, *Fibers Polymers*, **12**, 983 (2011).
24. K.- Zhong, Z. Man, Z. Huang, T. Chen, B. Yin and L. Yi Jin, *Polym. Int.*, **60**, 845 (2011).
25. H.A. Klok, J.J. Hwang, J.D. Hartgerink and S.I. Stupp, *Macromolecules*, **35**, 6101 (2002).
26. P. Xue, R. Lu, G. Chen, Y. Zhang, H. Nomoto, M. Takafuji and H. Ihara, *Chem. Eur. J.*, **13**, 8231 (2007).
27. H. Cho, L. Widanapathirana and Y. Zhao, *J. Am. Chem. Soc.*, **133**, 141 (2011).
28. M.F. Ottaviani, M. Cangiotti, L. Fiorani, A. Barnard, S.P. Jones and D.K. Smith, *New J. Chem.*, **36**, 469 (2012).
29. S. Tomas and L. Milanesi, *J. Am. Chem. Soc.*, **131**, 6618 (2009).
30. M. Banchelli, F. Betti, D. Berti, G. Caminati, F.B. Bombelli, T. Brown, L.M. Wilhelmsson, B. Nordén and P. Baglioni, *J. Phys. Chem. B*, **112**, 10942 (2008).
31. E. Ranucci, M.A. Suardi, R. Annunziata, P. Ferruti, F. Chiellini and C. Bartoli, *Biomacromolecules*, **9**, 2693 (2008).
32. S. Trachtenberg and R. Gilad, *Mol. Microbiol.*, **41**, 827 (2001).
33. A.H. Kycia, J. Wang, A.R. Merrill and J. Lipkowski, *Langmuir*, **27**, 10867 (2011).